# Highly flexible, transparent and low resistance IZO-Ag-IZO multilayer electrode for flexible OLEDs

[1]Sung-Woo Cho, [1]Kwang-Hyuk Choi, [1]Jin-A Jeong, [2]Se Hyung Lee, [2]Jang-Joo Kim, and [1]Han-Ki Kim *

[1]Dept. of Information and Nano-Material Engineering, Kumoh National Institute of Technology, 1 Yangho-dong, Gumi, Gyeongbuk 730-701, Korea
[2]Dept. of Material Science and Engineering, Seoul National University and Organic Light Emitting Diodes Center, Sillim-dong, Seoul 151-741, Korea
Phone: +82-54-7746, E-mail: hkkim@kumoh.ac.kr

**Keywords : IZO-Ag-IZO, PET, Surface plasmon resonance, Flexible OLEDs**

## Abstract

*Characteristics of indium-zinc-oxide (IZO)-Ag-IZO multilayer grown on a PET substrate were investigated for flexible organic emitting diodes. By inserting very thin Ag layer between amorphous IZO, IZO-Ag-IZO (IAI) multilayer anode exhibited remarkably reduced sheet resistance and high transmittance due to the surface plasmon resonance effect and Ag layer.*

## 1. Introduction

There is current considerable interest in flexible organic light emitting diodes (OLEDs) as a new generation displays due to their lightweight, robust, profile, ability to flex, curve, roll and fold for portability, and ultimate engineering design freedom. To fabricate high performance flexible OLEDs on poly substrate, highly flexible and transparent electrode on polymer substrate is necessary [1]. Recently Sn-doped $In_2O_3$ (ITO)-metal-ITO (IMI) multilayer have gained much attention as promising flexible anode materials for flexible OLEDs because the dielectric/metal/dielectric multilayer system an suppress the reflection from the metal layer and obtain a selective transparent effect [2].

In this work, we reports on characteristics of thin IZO (30 nm)-Ag (6~14 nm)-IZO (30 nm) multilayer anode grown on a PET substrate by using DC magnetron sputtering and thermal evaporation [3]. Using multilayer electrode with total thickness below ~70 nm, we can obtain high-quality flexible anode with very low sheet resistance and high transmittance comparable to amorphous ITO (a-ITO) anode prepared at room temperature. In addition, we show that IZO-Ag-IZO multilayer anode have good robustness under mechanical strain due to effect of the ductile Ag layer. Furthermore, we exhibits the integration of IZO-Ag-IZO anode with flexible OLEDs and demonstrates better electrical and optical performance of the flexible OLED than those of flexible OLED fabricated on the a-ITO/PET.

## 2. Experimental

The IZO-Ag-IZO multilayer anode was fabricated on 200 μm thick PET substrates using DC magnetron sputtering and thermal evaporation. Both top and bottom IZO films with thickness of 30 nm were deposited using DC magnetron sputtering at room temperature under identical condition. At a constant Ar flow rate of 20 sccm, DC power of 100 W, and a working pressure of 5 mTorr, 30 nm-thick IZO film were grown on a PET substrate with dimensions of 25 × 25 mm. After bottom IZO deposition, Ag films were deposited on the IZO film by thermal evaporator at a deposition rate of 0.02 nm/s. Ag film thickness was monitored with a quartz crystal microbalance during Ag deposition. Subsequently, 30 nm-thick top IZO film was deposited on evaporated Ag film by DC sputtering at identical deposition condition to the bottom IZO film. For comparison, a reference a-ITO/PET sample was prepared using DC sputtering at room temperature. Sheet resistance of IZO-Ag-IZO anode was measured at room temperature by means of four point probe as a function of Ag thickness. The transmittance of the IZO-Ag-IZO multilayer was measured in the wavelength ranges from 220 to 800 nm by a UV/visible spectrometer. To investigate the structural properties of the IZO-Ag-IZO multilayer, synchrotron x-ray scattering examinations were performed. Furthermore, the flexibility of the IZO-

Ag-IZO multilayer anode was analyzed by a laboratory made bending test system. The distance of stretched mode was 80 mm and that of bended position was 30 mm. The bending radius was approximated to 8 mm and the bending frequency was 1 Hz. During bending test, the resistance of the samples was measured by a multi-meter.

To compare electrical and optical properties of flexible OLED fabricated on IZO-Ag-IZO/PET and reference a-ITO/PET sample, we prepared standard flexible OLEDs on the IZO-Ag-IZO anode and reference a-ITO anode. After conventional wet cleaning and UV-ozone treatment for 10 min, both the IZO-Ag-IZO /PET and a-ITO/PET samples were transferred to an organic/metal evaporation system simultaneously. All organic layers were deposited by thermal evaporation in the following order: 40 nm-thick α-napthylphenlylbiphenyl (α-NPB) and 30 nm-thick 4,4'-bis(9-carbazolyl)-biphenyl (CBP) doped with 6 wt % [$Ir(ppy)_3$] were used as a hole transport layer (HTL) and a emitting layer (EL), respectively. Subsequently, a 10 nm-thick 2,9-dimethyl-4,7-diphenyl-1,10-phenanthroline (bathocuproine: BCP) layer was grown on the EL layer as a hole blocking layer (HBL). A 40 nm-thick tris-(8-hydroxyquinoline) aluminum ($Alq_3$) layer and a 1 nm LiF layer were then deposited as electron transport (ETL) and electron injection layers (EIL), respectively. Finally, a 100 nm-thick Al cathode layer was patterned using a shadow metal mask. After deposition of the Al cathode, the flexible OLED cells were encapsulated by same PET film to protect the flexible OLED cells from the moisture and the oxygen in air. Current density-voltage-luminance (*J-V-L*) characteristics of flexible OLEDs fabricated on different anode materials were measured with a Keithley 2400 and a Si photodiode mounted below the flexible OLEDs.

## 3. Results and discussion

Figure 1 shows the sheet resistance and transmittance of the IZO-Ag-IZO multilayer anode on a PET substrate as a function of average Ag thickness at constant thickness of IZO film (30 nm). It was shown that the sheet resistance of IZO-Ag-IZO multilayer significantly decreased with increasing Ag thickness. Above a thickness of 8 nm, the sheet resistance of IAI multilayer was rapidly decreased. In case of IAI multilayer with 14 nm-thick Ag layer, it shows sheet resistance of 5 Ω/sq. Sheet resistance dependence on thickness of Ag layer can be attributed to a transition from distinct island of Ag atoms to a continuous Ag films. The transmittance of IZO-Ag-IZO multilayer also depends on the thickness of Ag film. Figure 1 showed optical transmittance of IZO-Ag-IZO multilayer with increasing Ag thickness at 550 nm wavelength. At Ag thickness of 6 nm, it showed fairly low transmittance of 70.5 % due to the absorption in the aggregated Ag islands. However, at an Ag thickness of 12 nm, it showed the highest transmittance of 84.8 % due to the surface plasmon resonance effect of Ag layer. It was reported that the high index of refraction contrast between Ag and the dielectric layer result in efficient plasmon coupling and visible transparency greater than 90 % can be achieved [3]. Therefore, dramatically increased transmittance of IZO-Ag-IZO electrode with Ag thickness of 12 nm can be attributed to surface plasmon resonance (SPR) of properly designed Ag layer.

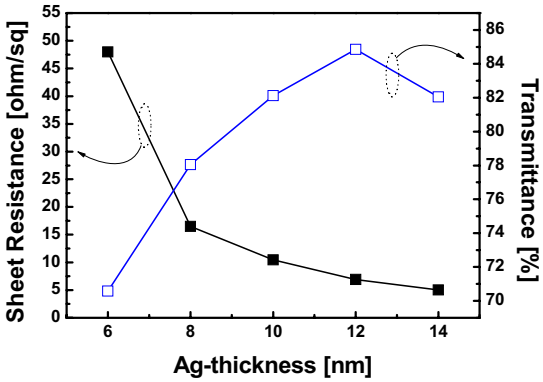


**Fig. 1. Sheet resistance and transmittance of IZO-Ag-IZO multilayer as a function of Ag thickness.**

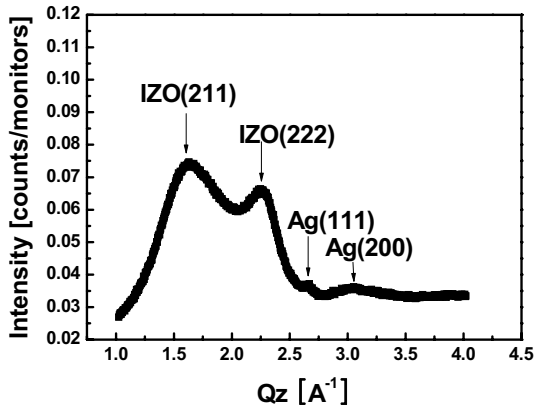


**Fig. 2. Synchrotron x-ray scattering plots obtained from optimized IZO-Ag-IZO anode on a PET substrate.**

Figure 2 shows typical θ-2θ scans result along the surface normal direction in reciprocal space [Q = 4πsin(2θ/2)/λ] of optimized IZO-Ag-IZO multilayer on a PET substrate with Ag thickness of 12 nm. The diffraction profiles of the optimized IZO-Ag-IZO multilayer exhibits four broad IZO and Ag peaks at Qz = 1. 62 [IZO (211)], 2.24 [IZO (222)], 2.65 [Ag (111)], and 3.06 [Ag (200)] indicative of amorphous structure. Due to the low PET substrate temperature during DC sputtering and evaporation process, both IZO and Ag films have an amorphous structure. In general, a-ITO prepared at room temperature has randomly distributed microcrystallines acting as source of film crack during film bending due to low amorphous/crystalline transition temperature ($T/T_m$< 0.19 ~ 150 °C). However, a-IZO film could maintain a stable amorphous structure below 500 °C due to high amorphous/crystalline transition temperature (~500°C) [4].

To investigate the flexibility of the optimized IZO-Ag-IZO multilayer prepared on PET substrate, a laboratory made bending test system were employed. Figure 3 shows change in resistance of both IZO-Ag-IZO/PET and a-ITO/PET with increasing bending cycles with inset of bending test system picture. The distance of stretched mode was 80 mm and that of bending position was 30 mm, i.e. the stroke of bending test was 50 mm. During the bending test, the resistance of the IZO-Ag-IZO/PET and a-ITO/PET sample was measured by a multi-meter. The change in resistance was expressed as [$R-R_0/R_0$], where $R_0$ is the initial resistance and R is the measured resistance after bending. It was shown that $R-R_0/R_0$ value of a-ITO/PET sample increase remarkably at initial bending cycles due to generation and propagation of cracks. However, IZO-Ag-IZO/PET sample exhibits constant $R-R_0/R_0$ value indicating constant resistance of IZO-Ag-IZO multilayer. The better robustness of IAI multilayer is attributed to existence of ductile Ag metal layer between IZO layers. Lewis *et al.* reported that ductile Ag layer between ITO layers provided effective electrical conductivity even after the ITO was beyond its failure strain (~0.8%) due to higher failure strain of bulk like Ag film (4~50 %) [2].

Figure 4 shows the current density-voltage-luminance (I-V-L) characteristics of flexible OLED fabricated on the IZO-Ag-IZO/PET and a-ITO/PET sample, respectively. It was shown that the current density of flexible OLED fabricated on the IZO-Ag-IZO multilayer anode is much higher than that of flexible OLED fabricated on a-ITO anode at same voltage after turn-on of flexible OLED. The higher current density of flexible OLED on the IZO-Ag-IZO multilayer anode in applied voltage is explained by different ohmic losses of IZO-Ag-IZO/PET and a-ITO/PET sample.

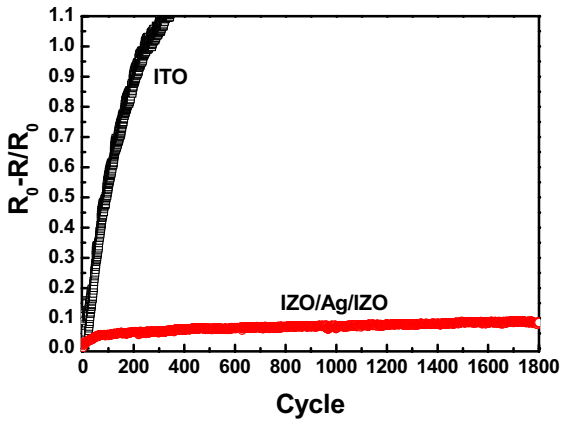


**Fig. 3. Normalized resistance change after repeated bending as a function of the number of cycles for IZO-Ag-IZO/PET and amorphous ITO/PET sample with inset of a laboratory made bending tester system.**

In addition, flexible OLED fabricated on a-ITO/PET sample exhibit a high leakage current at a forward bias before the turn of due to a large shunt resistance, indication leaky interface between the a-ITO and organic layer.

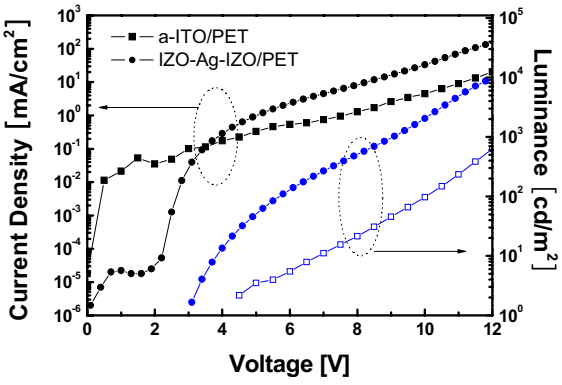


**Fig. 4. Current density-voltage-luminance (J-V-L) characteristics of flexible OLED fabricated on IAI/PET and a-ITO/PET sample,.**

While the flexible OLED on the IZO-Ag-IZO multilayer anode shows low leakage current density before turn-on of flexible OLED. The I-V curve of the flexible OLEDs on the IZO-Ag-IZO multilayer also exhibits much higher luminance than that of a flexible

OLED on the a-ITO/PET sample as expected from J-V curve [5].

## 4. Summary

We have demonstrated the applicability of IZO-Ag-IZO multilayer as an alternative to a-ITO anode prepared at room temperature. The IZO-Ag-IZO multilayer on a PET substrate showed low sheet resistance of 5 Ω/sq. and high transmittance of 84.8 % in spite of very thin thickness of IZO layer. The Ag metal layer with critical thickness of 12 nm sandwiched by amorphous IZO layer could provide significantly improved sheet resistance and transmittance as well as mechanical robustness upon bending. In addition, a flexible OLED fabricated on the IZO-Ag-IZO multilayer anode shows better current density and luminance than those of flexible OLED fabricated on a-ITO anode due to low sheet resistance and lower ohmic losses. This indicates that the IZO-Ag-IZO multilayer on polymer substrate is a promising flexible anode material that can be used as a substitute for a conventional a-ITO anode on polymer substrate.

## 5. References

1. J.-W. Kang, W.-I. Jeong, J.-J. Kim, H.-K. Kim, D.-G. Kim, G.-H. Lee, Electrochem. Solid-state Lett. 10 (2007) 75.
2. J. Lewis, S. Grefo, Chalamala, E. Vick and D. Temple, Appl. Phys. Lett. 85 (2004).
3. X. Liu, X. Cai, J. Qiao, J. Mao, and N. Jiang, Thin Solid Films 441, 200 (2003)
4. J. -H. Bae, J. -M. Moon, H. -K. Kim, J. -W. Kang, H. -D. Park, J. -J. Kim, and W. J. Cho, J. Electrochem. Soc. 154 (2007) 81.
5. S.-W. Cho, J.-A. Jeong, J.-H. Bae, J. M. Moon, and Han-Ki Kim, Thin Solid Films (in press)